Supplementary Material

Dynamin2 and Cortactin Regulate Actin Assembly and Filament Organization

Dorothy A. Schafer, Scott A. Weed, Derk Binns, Andrei V. Karginov, J. Thomas Parsons, and John A. Cooper

Supplementary Experimental Procedures

cDNAs, Proteins, and Reagents

Plasmids for expression of dynamin2aa and dynamin2aa (K44A) were gifts of Dr. Mark McNiven (Mayo Clinic, Rochester, MN), respectively [S1]. Plasmids for expression of FLAG-tagged mouse cortactin, N-terminal and C-terminal fragments of cortactin [S2], and FLAG-tagged cortactin (W525K) [S3] were as described. FLAG-tagged cortactin (W22A) was generated by mutating pFLAG-cortactin with primer pairs 5′-GGAGGAGCTGATGACGCGGAGACTGATC CTG-3′ and 5′-CAGGATCAGTCTCCGCGTCATCAGCTCCTCC-3′ with the QuickChange site-directed mutagenesis kit (Stragagene). Plasmids for expressing the HA-tagged SH3 domain of amphiphysin1 and a control plasmid for expression of the HA-tagged mutant form of the amphiphysin1 SH3 (G684R, P687L) domain were gifts of Dr. Pietro DeCamilli (Yale University, New Haven. CT).

Actin was purified from chicken pectoral muscle [S4] and filtered on Sephadex G150; pyrene-labeled actin was prepared as described [S5]. GST-cortactin was expressed in bacteria, and cortactin was purified as described [S2], with the following modifications. Following proteolytic cleavage by Tev protease (BRL) to remove the GST, cortactin was purified by anion exchange chromatography on MonoQ resin. Recombinant His-tagged bovine dynamin2aa was expressed in Sf9 insect cells infected with baculovirus and was purified as described [S6]. Arp2/3 complex was purified from bovine calf thymus as described [S7]. GST-VCA, a fusion protein of GST and the C-terminal region of human N-WASp [S8], was expressed in *E. coli* and was purified by using affinity on glutathione-agarose. Rhodamine-phalloidin was purchased from Molecular Probes; GTP and GTPγS were purchased from Calbiochem. Phospholipids were purchased from Avanti Polar Lipids. Lipid stock solutions were prepared at a concentration of 1 mM in 20 mM imidazole (pH 7.0), 50 mM KCl, and 1 mM EDTA. Lipid preparations were subjected to five cycles of freeze/thaw in a dry ice-ethanol bath, followed by sonication in a bath sonicator for 90 s. Rabbit antibodies to the PRD of dynamin2 were a kind gift of Dr. Pietro DeCamilli [S9]. Monoclonal anti-dynamin2 used in immunoblots was purchased from Transduction Labs.

Cell Culture, Transfection, and Immunocytochemistry

PtK1 cells stably expressing GFP-CP were isolated and maintained as described [S10]. To express exogenous proteins, nuclei were injected with plasmid DNA (20–30 μg/ml) mixed with rhodamine-dextran to mark injected cells. Control cells were mock transfected by injecting pcDNA3-FLAG, the plasmid used for constructing plasmids to express cortactin. Video recordings of injected cells were collected 3–5 hr after injection as described [S10]. Immunofluorescence localization of dynamin in cells expressing GFP-CP was carried out as described [S10].

Quantitative Analysis of Actin Dynamics In Vivo

To quantify actin dynamics at foci in live cells, we measured the fluctuation of the GFP-CP fluorescence over time in regions of well-spread, flat lamellae. A temporal and spatial fluctuation function was defined based on the Fourier components of the fluorescence intensity of GFP-CP. The Fourier components of the GFP-CP fluorescence are defined as follows:

$$I(q_x,q_y,\omega) = \sum_{i_x,i_y,t} \exp i(-q_x i_x - q_y i_y + \omega t), \quad (1)$$

where i_x and i_y are the pixel indices in the images and t is the number of a frame in the video sequence. The Fourier components are defined for a discrete set of $q-$ and $\omega-$ values given by $q_x = 2\pi m_x/L$ ($0 \le q_x$, $L - 1$), $q_y = 2\pi m_y/L$ ($0 \le q_y \le L - 1$), and $\omega = 2\pi mt/T$ ($0 \le mt \le T - 1$), where L is the size of the image measured in pixels and T is the number of frames in the observation period. The temporal-spatial fluctuation function is then defined as:

$$F = \sum_{q_x,q_y,w} |I(q_x,q_y,\omega)|^2/|I(0,0,0)|^2/, \quad (2)$$

where the summation is restricted by the conditions:

$$q^2_{min} \le (q^2_x + q^2_y) \le q^2_{max}$$

$$\omega_{min} \le \omega \le \omega_{max}.$$

The function F (Equation 2) measures the extent of intensity fluctuations in the wavelength and frequency ranges defined by q_{min}, q_{max}, q_{min}, and ω_{max}. If $q_{min} > 0$ and $\omega_{min} > 0$, then F will vanish for a dataset that is constant in time or space. The cutoffs q_{max} and ω_{max} are used in order to limit contributions from noise in the images. We used the following values of the parameters: $q_{min} = 0.0628$, $q_{max} = 0.628$, $\omega_{min} = 50$, and $\omega_{max} = 300$.

Three to seven regions in well-spread lamella were selected for analysis. In most cases, an observer with no knowledge of the identity of control or experimental cells selected the regions to be analyzed. Between 5 and 22 cells were analyzed for each experimental condition. The fluctuation function was evaluated with cells treated with Latrunculin B or cells expressing dominant-negative Rac1,

Table S1. Identification of Rab6-Interacting Proteins in Rat Liver Cytosol

Protein	Score	Sequence Coverage (Percent)	Number of Peptides
p150^{glued}	4.9×10^{-4}	21	22
BICD2[a]	0.24	15	18
R6IP2	2.5×10^{-4}	19	20
REP-1	0.54	22	10
Rab-GDI-3[b]	1.9×10^{-4}	37	17

Allowing for partial oxidation of methionine residues, complete modification of cysteine by iodoacetamide during sample preparation, and single missed trypsin cleavages, we performed searches of monoisotopic peptide masses. We set tolerance to 50 parts per million to allow for errors in peptide mass determination.

[a] This match is to human BICD2 because no rat sequence is present in the databank.

[b] This match is to mouse Rab GDI-3.

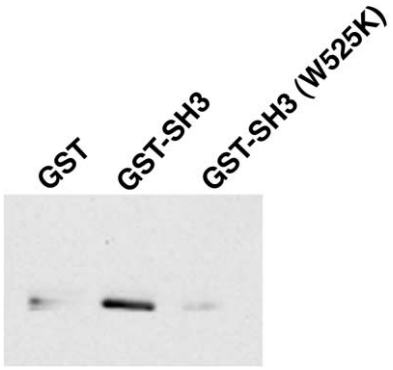

Figure S1. A Mutation in the Cortactin SH3 Domain Disrupts Dynamin2 Binding

GST fusion proteins containing amino acids 483–546 of cortactin were tested for their ability to bind dynamin2. Dynamin2 at 50 nM was incubated for 2 hr at 4°C with 20 μl glutathione-agarose beads containing 10 μg GST, GST-cortactin SH3, or GST-cortactin SH3 (W525K) in 10 mM Tris-Cl (pH 7.4), 5 mM $MgCl_2$, 0.2 mM EDTA, and 50 mM NaCl. Beads were washed three times in the binding buffer, and bound dynamin was identified on Western blots using anti-dynamin2.

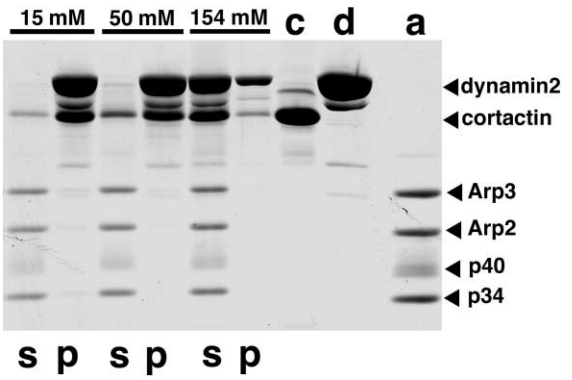

Figure S3. Cortactin, but Not Arp2/3 Complex, Assembles with Oligomeric Dynamin2

Dynamin2 and cortactin cosedimented in 15 mM KCl and at 50 mM KCl, ionic conditions that promote dynamin assembly; at 154 mM KCl, which provides less assembly, dynamin2 and cortactin were primarily in the supernatant fraction. Arp2/3 complex remained in the supernatant fraction at all salt concentrations. In control reactions without dynamin2, neither Arp2/3 complex nor cortactin were detected in pellet fractions (data not shown). Reactions contained 525 nM dynamin2, 511 nM cortactin, and 100 nM Arp2/3 complex in varying concentrations of KCl in 20 mM HEPES (pH 7.0), 2 mM EGTA, 1 mM $MgCl_2$, and 0.1 mM DTT. Samples were incubated for 10 min at room temperature, followed by centrifugation at 100,000 × g for 10 min (Beckman TLA 120.1 rotor). SDS gel samples of the supernatant and pellet fraction were prepared as described [S12]. A Coomassie blue-stained 10% polyacrylamide gel shows proteins obtained in the supernatant (s) and pellet (p) fractions. Lanes labeled c, d, and a show the cortactin, dynamin2, and Arp2/3 complex, respectively, used in the reactions. Only the four largest subunits of Arp2/3 complex (Arp3, Arp2, p40, and p34) remained on the 10% gel.

treatments that completely abolish actin assembly by different mechanisms; these treatments decreased the fluctuation of GFP-CP fluorescence to near zero, as expected.

Quantitation of Morphology and Dynamics of Individual Foci

The rate of foci movement, the duration of movement, and the length of foci were quantitated with tools provided in NIH Image to record x,y coordinates of the leading tip of moving foci in several frames of a movie. Data were collected from at least 8 foci in 2–3 cells.

Actin Assembly Assays

Actin assembly with purified proteins was quantified by using fluorometric assays with pyrene-actin [S5]. Reactions contained 2.0 μM actin (10% pyrene-labeled actin), 50 nM Arp2/3 complex, 90–400 nM cortactin, varying concentrations of dynamin2, 15 μM phospholipid vesicles (90:10 mol:mol PC:PIP_2 or PC) in 20 mM imidazole (pH 7.0), 1 mM EGTA, 2 mM $MgCl_2$, and 50 mM KCl (MKEI buffer).

Light Microscope Assay of Actin Filament Organization

Visual observations of the actin filaments formed in reactions containing Arp2/3 complex, cortactin, and dynamin2 were performed by a modification of the method described by Blanchoin et al. [S11]. Reactions contained 62 nM Arp2/3 complex, 450 nM cortactin, 450 nM dynamin2, 2 μM actin in MKEI buffer, and 50 μM phospholipid vesicles (PC or PC:PIP_2, 90:10 mol:mol). Phospholipid preparations

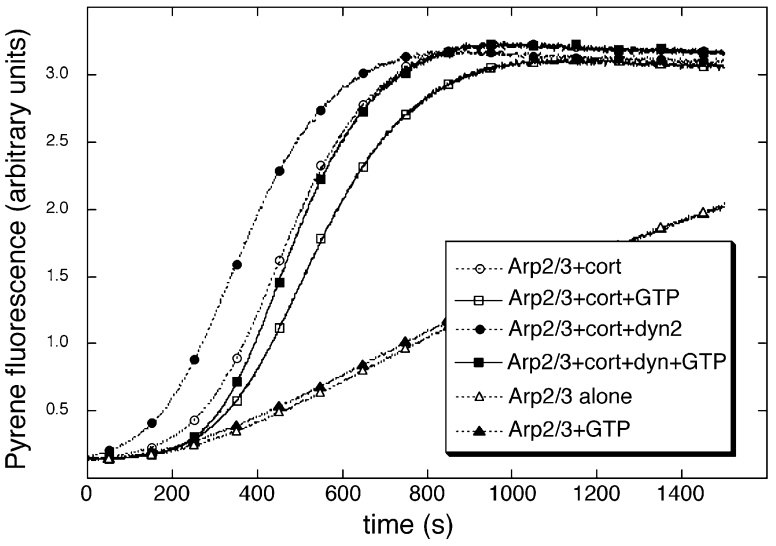

Figure S2. Effect of GTP on Actin Assembly by Arp2/3 Complex, Cortactin, and Dynamin2

GTP (200 μM) had no effect on enhanced actin nucleation by 33 nM dynamin2. Reactions contained 50 nM Arp2/3 complex, 90 nM cortactin, and 15 μM PC:PIP_2 (90:10 mol:mol) in the presence or absence of 33 nM dynamin2 and/or 200 μM GTP, as indicated in the legend. The fluorescence of pyrene actin is plotted over time. GTP reduced the rate of actin assembly in reactions containing only Arp2/3 complex and cortactin, but the enhanced actin nucleation by dynamin2 was similar to that observed in the absence of GTP.

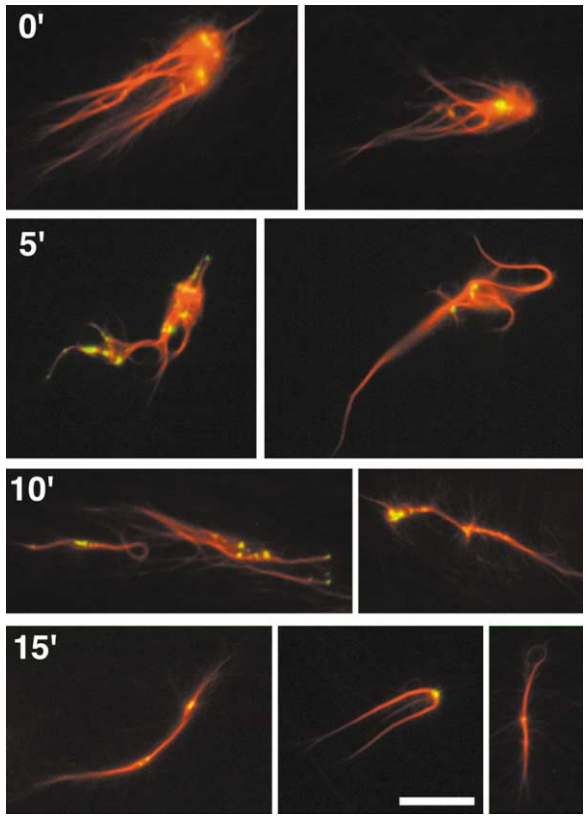

Figure S4. Dynamin GTPase Activity Alters the Organization of Lipid and Actin Filaments

The images illustrate the time course for the effects of GTP on the organization of actin filaments associated with PC:PIP_2-containing vesicles formed in reactions of actin, Arp2/3 complex, cortactin, dynamin, and PC:PIP_2-containing vesicles in MKEI buffer. GTP (200 μM) was added after 10 min, a time when lipid aggregates with associated actin filaments similar to those shown in Figures 3B and 3D had formed (0 time point). Representative views of the lipid-actin filament structures formed 5 min, 10 min, and 15 min after the addition of GTP are shown. Actin filaments and lipid vesicles were visualized with rhodamine-phalloidin and fluorescein-PE, respectively, as described in the Experimental Procedures. The scale bar represents 10 μm.

contained a trace amount (1%) of fluorescein-labeled phosphatidylethanolamine to visualize the lipid vesicles. GST-VCA was used at 1.5 nM. Reactions were carried out in the absence of rhodamine-phalloidin; at each time point, an aliquot of the reaction was removed and gently mixed with an equal volume of 8 μM rhodamine-phalloidin in MKEI buffer. Rhodamine-phalloidin-labeled filaments were subsequently diluted in mounting buffer (MKEI buffer containing 100 mM DTT, 20 μg/ml catalase, 100 μg/ml glucose oxidase, 0.4% (w/v) methylcellulose, and 3 mg/ml glucose), mounted on poly-lysine-coated coverslips, and observed with epifluorescence microscopy.

Supplementary References

S1. Cao, H., Thompson, H.M., Krueger, E.W., and McNiven, M.A. (2000). Disruption of Golgi structure and function in mammalian cells expressing a mutant dynamin. J. Cell Sci. *113*, 1993–2002.

S2. Weed, S.A., Karginov, A.V., Schafer, D.A., Weaver, A.M., Kinley, A.W., Cooper, J.A., and Parsons, J.T. (2000). Cortactin localization to sites of actin assembly in lamellipodia requires interactions with F-actin and the Arp2/3 complex. J. Cell Biol. *151*, 29–40.

S3. Du, Y., Weed, S.A., Xiong, W.C., Marshall, T.D., and Parsons, J.T. (1998). Identification of a novel cortactin SH3 domain-binding protein and its localization to growth cones of cultured neurons. Mol. Cell. Biol. *18*, 5838–5851.

S4. Spudich, J.A., and Watt, S. (1971). The regulation of rabbit skeletal muscle contraction. J. Biol. Chem. *246*, 4866–4871.

S5. Bryan, J., and Coluccio, L.M. (1985). Kinetic analysis of F-actin depolymerization in the presence of platelet gelsolin and gelsolin-actin complexes. J. Cell Biol. *101*, 1236–1244.

S6. Lin, H.C., Barylko, B., Achiriloaie, M., and Albanesi, J.P. (1997). Phosphatidylinositol (4,5)-bisphosphate-dependent activation of dynamins I and II lacking the proline/arginine-rich domains. J. Biol. Chem. *272*, 25999–26004.

S7. Higgs, H.N., Blanchoin, L., and Pollard, T.D. (1999). Influence of the C terminus of Wiskott-Aldrich syndrome protein (WASp) and the Arp2/3 complex on actin polymerization. Biochemistry *38*, 15212–15222.

S8. Egile, C., Loisel, T.P., Laurent, V., Li, R., Pantaloni, D., Sansonetti, P.J., and Carlier, M.F. (1999). Activation of the CDC42 effector N-WASP by the Shigella flexneri IcsA protein promotes actin nucleation by Arp2/3 complex and bacterial actin-based motility. J. Cell Biol. *146*, 1319–1332.

S9. Lee, E., and De Camilli, P. (2002). Dynamin at actin tails. Proc. Natl. Acad. Sci. USA *99*, 161–166.

S10. Schafer, D.A., Welch, M.D., Machesky, L.M., Bridgman, P.C., Meyer, S.M., and Cooper, J.A. (1998). Visualization and molecular analysis of actin assembly in living cells. J. Cell Biol. *143*, 1919–1930.

S11. Blanchoin, L., Amann, K.J., Higgs, H.N., Marchand, J.B., Kaiser D.A., and Pollard, T.D. (2000). Direct observation of dendritic actin filament networks nucleated by Arp2/3 complex and WASP/Scar proteins. Nature *404*, 1007–1011

S12. Damke, H., Binns, D.D., Ueda, H., Schmid, S.L., and Baba, T. (2001). Dynamin GTPase domain mutants block endocytic vesicle formation at morphologically distinct stages. Mol. Biol. Cell *12*, 2578–2589.

Movie 1. Actin Dynamics in a PtK1 Cell Observed with GFP-Capping Protein

The dynamic distribution of GFP-capping protein (GFP-CP) in a PtK1 cell reveals sites of actin assembly at the cell periphery and at focal sites (foci) within the lamella proximal to the leading edge. Video data were recorded for 2 min, and the rate of playback is 20× real time.

Movie 2. Actin Dynamics in a PtK1 Cell Expressing Dynamin2

The dynamic distribution of GFP-CP at foci and at the cell periphery in a PtK1 cell expressing wild-type dynamin2 appears similar to that in control, mock-transfected cells. Video data were recorded for 2 min, and the rate of playback is 20× real time.

Movie 3. Actin Dynamics in a PtK1 Cell Expressing Dynamin2 K44A

The dynamic distribution of GFP-CP in cells expressing dynamin2 K44A differs from control cells in that foci are longer and dynamic, bright punctate structures of GFP-CP appear. Video data were recorded for 2 min, and the rate of playback is 20× real time.